BioChip J. (2015) 9(1): 50-58
DOI 10.1007/s13206-014-9107-x

Original Article

Investigation of Bacterial Chemotaxis Using a Simple Three-Point Microfluidic System

Hoyeon Kim[1], Jamel Ali[1], Kiran Phuyal[1], Sungsu Park[2] & Min Jun Kim[1,3,*]

Received: 03 December 2014 / Accepted: 14 January 2015 / Published online: 10 March 2015

Abstract A three-point microfluidic system was developed and used to experimentally verify bacterial chemotaxis with known chemoeffectors. Using pneumatically-controlled micro-valves, the device was able to regulate microscale flows and created concentration gradients that allowed GFP-labelled *Escherichia coli* cells to interact with an environment that contained a chemoattractant and a chemorepellent. Having two separate possible paths (left and right) for the bacteria to move forward, this device also allowed for imaging processing based removal of noisy data, if adirectional bias was present. This device could be useful for quantitative analysis of chemotactic behaviors with minimal technical requirements, and could motivate the development of future devices based on this concept.

Keywords: Bacterial Chemotaxis, Microfluidics, Bacterial Motility, *Escherichia coli*, Microfluidic gradient

Introduction

Microfluidics has begun to have a major impact on microbiology. Microfluidics is a unique technology that allows for manipulation of very small volumes (10^{-9} to 10^{-18} liters) of fluids in micron-scale channels with high precision[1]. This ability of microfluidic technology to use minute quantities of samples and reagents enables the separation and detection of analytes with high resolution and sensitivity. The ultra-low cost associated with device fabrication along with other advantages, such as reduced reaction time, very low sample requirements (e.g. reagents, solvents, cells), high through-put screening, portability, ability to be customized with versatile designs, and the potential to be integrated with other miniaturized devices, have made microfluidic technology an attractive alternative to traditional laboratory techniques[2-5]. Microfluidics is expected to bridge the gap between biologists who study microbial life, and engineers who develop the technology to build microstructures[6]. In the past decade, the concept of lab-on-the-chip has gained wider recognition among scientists and engineers, and it is progressing at an unprecedented rate. This collaborative effort between microbiologists and microelectromechanical systems (MEMS) engineers is already having a major impact in single-cell analysis, genomics research, molecular analysis, bio-defense, molecular biology, microcommunication, and microelectronics[1,6,7].

Microfluidic devices are increasingly being used to study cellular migration behavior, such as chemotaxis, because of their ability to regulate, configure, and flexibly manipulate chemical concentration gradients in local cellular environments. This helps in mimicking and replicating naturally occurring *in vivo* microenvironments[8,9]. The cellular environment is very complex with numerous physical and biochemical signals. There exist numerous complex interactions (chemotaxis, aerotaxis, thermotaxis etc.) between cells and their surroundings. Investigation of such behavior is important to understanding the underlying mechanisms at the molecular level. Utilizing chemotaxis, cells are able to regulate their motility behavior in response to gradients of chemical signals that are present in the cellular mi-

[1]Department of Mechanical Engineering and Mechanics, Drexel University, Philadelphia, Pennsylvania 19104, USA
[2]School of Mechanical Engineering, Sungkyunkwan University, Suwon 440-746, Korea
[3]School of Biomedical Engineering, Science and Health Systems, Drexel University, Philadelphia, Pennsylvania 19104, USA
*Correspondence and requests for materials should be addressed to M.J. Kim (✉mkim@coe.drexel.edu)

croenvironment[9,10]. This is critical in the survival of microorganisms, as chemotaxis enables populations of these organisms to collectively locate and optimize their energy and resources. The chemical signals generated in microenvironments, due to complex biochemical phenomena, play a major role in many microbial processes, such as biofilm formation, disease pathogenesis, wound healing, contaminant bioremediation, cellular differentiation, and growth[10,11]. By controlling the spatiotemporal characteristics of local environments, the innate chemotactic behavior of eukaryotes and prokaryotes can be studied and quantified in miniature microfluidic devices[12].

Prokaryotic flagellated bacteria have chemoreceptors in their cell membrane that help them detect a wide range of signals such as concentrations of nutrients, toxins, oxygen levels, osmolality, and pH in their microenvironments[13]. Bacterial cells, in response to these signals, show chemotactic responses in which their net migration is biased towards the chemoattractants (that enhances the survival) and away from chemorepellents (that endangers the survival)[14]. In a uniform environment flagellated bacterial cells, such as *Escherichia coli* (Figure 1), swim at speeds of ~30 μm/sec by rotating their left-handed flagella bundles in alternating clockwise (CW) and counter-clockwise (CCW) directions using bidirectional, ion-driven rotary motors[12,15]. This CCW rotation leads to a steadily forward motion that lasts for about 1 sec, which is commonly referred to as "run". Towards the end of the "run" cycle, the flagellar bundle unravels and the flagellar filaments start to work independently leading to erratic motion with very low net displacement. This motion lasts for about 0.1 sec, and is commonly referred to as "tumble"[16]. This alternating run and tumble motion leads to a three-dimensional random walk. It is widely accepted that this switching between the CW and CCW direction involves the proteins FliG, M, and N. In absence of chemical gradients, the cell undergoes random walks with alternating run and tumble cycles[17,18]. But in presence of chemical gradients, temporal changes in concentration are detected by chemoreceptors through differentiation of the instantaneous concentrations during very short time periods (seconds)[12]. The flagellated bacteria can purposefully modify its runs and tumbles through activity proteins (e.g. FliG, M, and N) that themselves actively respond in the presence of chemoreceptors. Eventually the cells can move towards or away from a chemical gradient in their microenvironment by biasing their movement[17,18]. Bacterial chemotaxis have been conventionally studied by using swarm plate assays, capillary assays, temporal gradient assays, three-dimensional tracking of cells using Berg's technique, and cell tethering techniques[4]. But in recent times

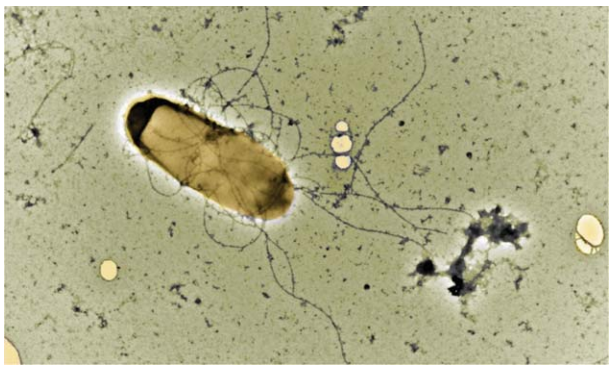

Figure 1. False-color TEM image of flagellated *Escherichia coli*.

microfluidic approaches have become more popular because of their advantages. Broadly, the microfluidic approach can be categorized into two groups based on the method they employ to generate chemical gradients, i.e. flow-based and diffusion -based devices[19,20]. Because of the micron-scale size of the devices, the flow is usually laminar at low Reynolds number regime. As the name suggests, flow-based devices use flow manipulation techniques, such as distribution channels and pneumatic valves, to generate diffusive patterns of various concentrations[21-23]. But the shear stress and removal of local chemical species can potentially alter chemotactic responses in flow-based devices. Also several studies have shown that the motility is also affected due to the shear stress induced upon the cells[10]. Diffusion-based gradient generators use the inherent diffusive property of chemoeffectors that diffuse freely across rigid membranes and hydrogel barriers to create gradients, or by stopping flow of two parallel streams using micromanipulation techniques such as electrophoresis and incorporation of pneumatic valves[10,24-26]. Diffusion-based devices eliminate flow-induced flaws in chemotactic experiments but are limited because of the need to account for the differences in the diffusion coefficients of each chemical species for each experiment. Since the diffusion coefficient is an inherent property, it is not easy to design a single device to accommodate for a wide range[10].

Here we use a microfluidic device based on the stopped flow principle to generate chemoeffector gradients. Using a valve system, a static fluidic environment was created after the chemoattractant (L-aspartate) or chemorepellent ($NiSO_4$) were introduced in the main channels. These chemoeffectors have similar diffusion coefficients (~70-80 μm^2/sec), and are known chemoeffectors in the scientific community[15]. GFP-labelled *E. coli* cells were used in this experiment, and the responses were captured using a high resolution CCD

camera. Once the bacteria are introduced into the fluidic environment, using micro-valve controlled flow, their net movement was recorded. The chemotactic behavior of these bacteria was subsequently characterized by using the image processing capabilities of MATLAB.

Results and Discussion

Device design concept

The Reynolds number (*Re*) is used to characterize fluid flow. It can be calculated by

$$Re = (\rho v D)/\mu \quad (1)$$

where ρ is the fluid density, v is the characteristics velocity of fluid, D is the hydraulic diameter, and μ is the viscosity of the fluid. For a microchannel 100 μm in width and 30 μm in height, the Reynolds number is much smaller than 1. Hence the flow is laminar[27].

The concept of this device is to utilize pneumatic microvalves to create a chemical gradient using a stopped flow. The device aims to use the diffusive gradient developed by the stopped flow for testing the chemotactic ability. As shown in Figure 2, the main experimental area consists of triangular shaped channels with access to three microvalve regulated microchambers that delivers the required chemoeffectors and bacterial cells.

Although this experiment is focused on using diffusion of single chemical species from two chambers on one bacterial species at a time, the designed devices could be utilized to investigate the effect of two different chemical species, loaded in two different chambers, on bacterial chemotaxis. This allows for simultaneous observation of biased motility, requiring only a minor modification in design parameters (such as length of the channel) to accommodate for differences in the diffusion coefficient. Similarly, this device could also be used to test the behavior of two groups of bacteria simultaneously in response to the gradient of a single chemoeffector.

Device simulation

Simulation methods, such as the finite Element Method, have been used to characterize flows, mixing processes, characterize and evaluate design performance of device with dynamic parameters because numerical simulation allows the researchers to determine how different parameters affect the performance[28-31]. By doing so the prototype iterations could be minimized and important insights about the device could be obtained. The ability to solve for gradient boundary conditions, including phase transfer encountered during the device usage, has made finite element method an attractive tool for device characterization[31].

For this experiment, the diffusion inside of the three chambers were modelled using the diffusive flow model. The device parameters followed the actual device

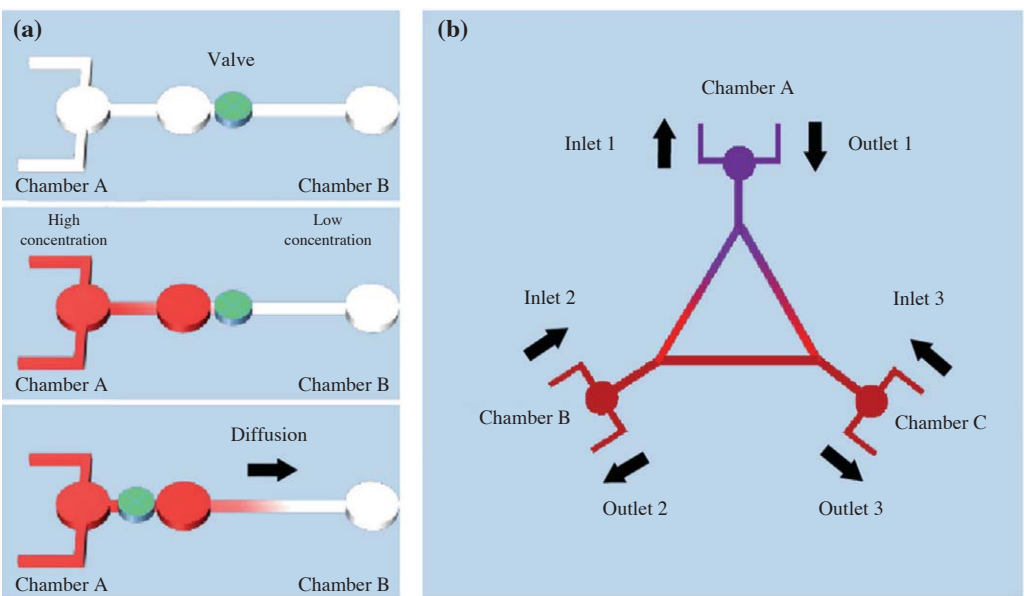

Figure 2. (a) Once chamber A is filled with solution, the valve is opened so that the net diffusion of chemicals is from Chamber A (higher concentration) to Chamber B (lower concentration). The manipulation of pneumatic fluid prevents the backflow. (b) Incorporation of 3 chambers in which now there is a net diffusion from of chemicals at higher concentration from chamber B and C to A.

dimension with channel height of 30 μm, diffusion coefficient of 5×10^{-10} m^2/sec, and initial concentration of 0.5 mol/ m^3. Initially the two chambers are filled with the chemicals at initial concentration of 0.5 mol/m^3 while the third channel had a net concentration of zero. In order to maintain a uniform supply of chemicals in the chambers, a laminar micro-flow was introduced that supplied the two chambers with chemicals at the concentration of 0.5 mol/m^3 of chemoeffector, while the third chamber supplied deionized (DI) water. Since the inlet volume equals to outlet volume, there is no net convective flow and the mass transfer was only due to diffusion.

As shown in Figure 3, there was a net diffusion of chemoeffectors from higher concentration to lower concentration. If chemoattractants are released from two chambers and the bacteria are released from the third, it can be expected that the rate of movement of bacterial cells would be higher. Conversely, if chemorepellents are being released, the opposite result would be expected.

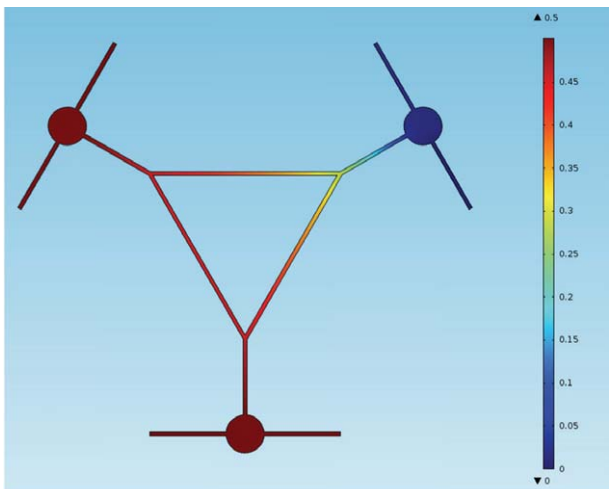

(color bar: mol/m^3)

Figure 3. Simulation result showing the diffusive mass transfer from a region of higher concentration to lower concentration (0.5 mM (red) to 0 mM (blue)).

Motility characterization

Motility parameters were characterized by using Region Based Tracking method. Using a pipette, about 10-20 μL of motility buffer (0.01 M Potassium Phosphate buffer, 0.067 M Sodium Chloride, 10^{-4} M EDTA, pH 7.5) was mixed with a drop of cultured bacterial cells that were extracted at their exponential phase. The drop was then used to make a wet mount slide for imaging. A phase-contrast microscope equipped with a high speed camera was used to take videos at 100 frames/sec for about 10 sec. The videos obtained were converted to binary images. The threshold value was found by random trial and error such that background noise was minimized. By using the positional value based on the centroid of object's pixel area, the motion of bacterial cells were tracked in two-dimensional space for the video sequence to generate motion trajectory[16].

Bacterial motion in absence of chemical gradients is described as a purely diffusive process. It is defined as $D=\langle r^2 \rangle / \Delta t$ where $\langle r^2 \rangle$ is the mean square displacement and Δt is the time interval. By calculating the mean square displacements in two-dimensional space and using the Δt as 0.01 sec, the diffusion coefficient was calculated from the average for the bacterial population.

As shown in Figure 4(a), the cells trajectories were used to calculate the diffusion coefficients. The diffusion coefficient was calculated to be 7.76×10^{-9} m^2/sec for *luxS* mutant and 9.56×10^{-9} m^2/sec for *lsrK* mutant.

This is comparable to diffusion coefficients found in literature for *E. coli*, which can range from 4×10^{-10} m^2/ sec for wild type *E. coli* K-12 and 2×10^{-9} m^2/ sec

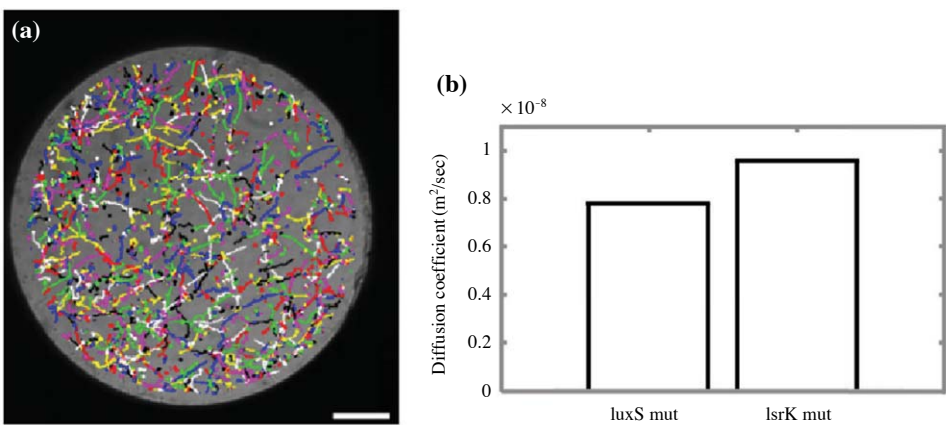

Figure 4. (a) Cell trajectory of multiple bacterial cells being tracked at the same time. (b) Diffusion coefficient of *E. coli* cells.

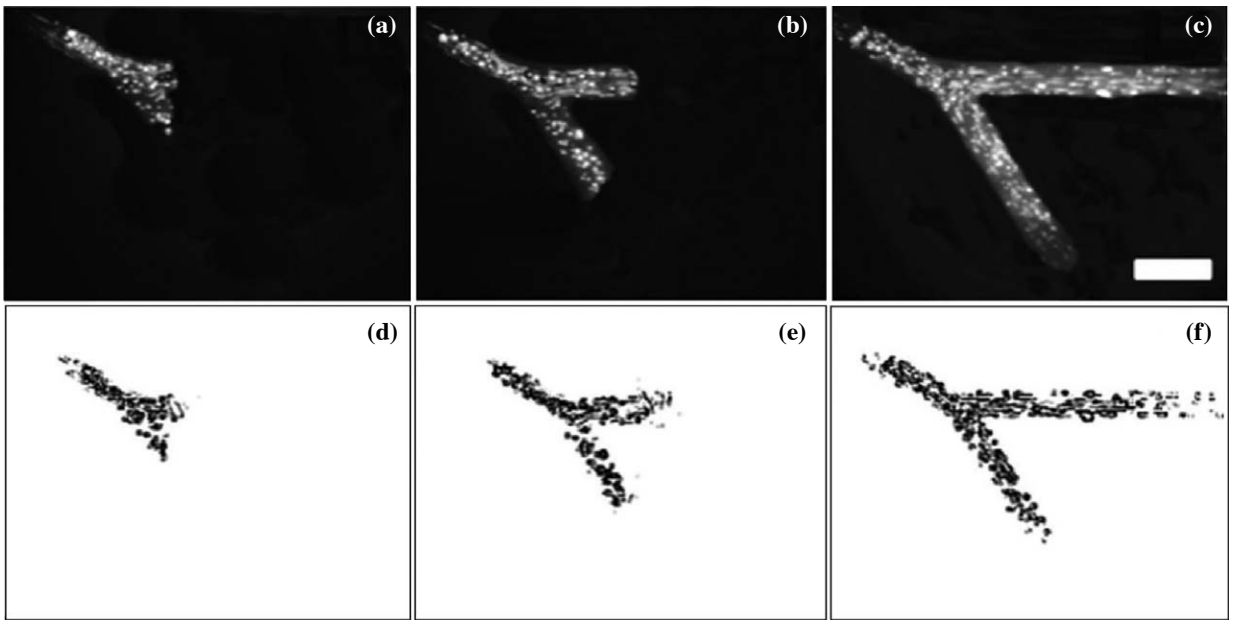

Figure 5. Images of *E. coli* luxS cells showing chemotaxis behavior. (a) After ~2 min, (b) After ~7 min, (c) After ~20 min, (d-f) corresponding binary conversion for images in (a-c). After the first 1 mm at which the cells reaches the two-way junction, the distance is averaged to obtain the time taken to reach. Scale bar 250 μm.

for smooth swimming mutant variation of *E. coli*[32]. This shows that the two strains of *E. coli* are highly motile.

After determining diffusion coefficients, chemotaxis experiments using our triangular device were conducted. First, one chemoeffector of a certain concentration was injected into two of the loading chambers, after which a fixed bacteria population, ~1.5×10^8 cells/mL, was loaded into the remaining empty chamber. The valves connecting each chamber were then opened and chemotaxis behavior was observed. In order to characterize the chemotaxis, a image processing technique was used in which the images were converted to grey-scale image to determine the position. As compared to the intensity based prediction, in which the fluorescence intensity is measured to predict the location, this process of image conversion to measure the diffusion distance was used because cells had variable speed. In this experiment only the bulk bacterial population was tracked in one z-plane as the presence of outliers (bacteria which had higher linear displacement) and/or movement of bacteria in the z-direction could skew the result due to large intensity differences.

As shown in Figure 5, the images of the cells movement were captured, and the time taken to reach the distances were determined. The positional markers were used to estimate the distance of travel. The first wave of bacterial cells were used to determine the relative time taken by a population to reach the end of a channel. Before the start of the main chemotatic investigation, a similar experiment was done in which the bacterial cells were allowed to diffuse freely. This was used as a point of reference. Next, four different concentrations of a certain chemoeffector, either L-aspartate (chemoattractant) or Nickel Sulfate (chemorepellent), were prepared, ranging from 30 mM to 100 mM.

It is important to note that like any biological systems, there is a wide variation in bacterial motility. Even with the same nutrients, temperature, pH, and all other conditions, there was wide variation in motility of bacterial cells. Hence, in order to characterize any biasness in motion, the following parameter was defined:

$$\psi = (t/t_o) \tag{2}$$

where t=time taken to reach fixed point in presence of chemoeffectors, and t_0 is the time taken to reach the same point in absence of chemoeffectors.

Before the start of every experiment, each group of *E. coli* cells were allowed to diffuse freely in absence of chemoeffectors. The time period to reach 0.5 mm, 1 mm, 1.5 mm, and 2 mm were noted as t_0 for those respective points. This was used as a calibration unit. This implies that if the parameter ψ was less than 1 than the positive chemotaxis was observed as the bacterial cells were able to reach faster in the same position. Conversely the value of greater than 1 implied that the negative chemotaxis was observed because it

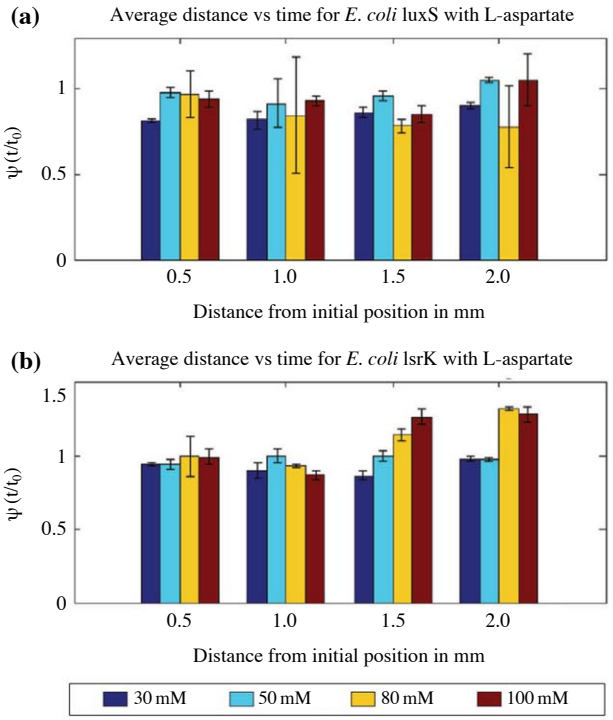

Figure 6. (a) *E. coli* luxS mut response to l-aspartate and (b) *E. coli* lsrK mut response to l-aspartate.

took longer time to reach the same position.

As shown in Figure 6(a) and (b), addition of L-aspartate led to a slight decrease in the time required to reach the marked positions, indicating that positive chemotaxis was observed. This is due to bacteria biasing their random walk to more translational movement ('runs') towards regions of higher concentration of L-aspartate. This increasing movement up an attractant gradient is known to be caused by a series of protein network interactions, triggered by the adsorption of aspartate on membrane bound receptor proteins that leads to the flagellar motor turning more counter-clockwise that clockwise[33]. The increased counter-clockwise motion of the motor causes bacterial flagella to bundle more, leading to forward thrust. However for the L-aspartate concentrations used relatively small fluctuations in chemotactic response were observed. It has been reported that the aspartate receptors of *E. coli* can be saturated, at L-aspartate concentrations as low as 1 mM, leading to a decrease in bacterial motility towards the attractant gradient[33,34]. Therefore the relatively high L-aspartate concentrations used may have had an abnormal effect on the positive chemotaxis, such as repulsion, due to chemoreceptor saturation.

The same process was repeated with Nickel Sulfate, a known chemorepellent, as shown in Figure 7(a) and

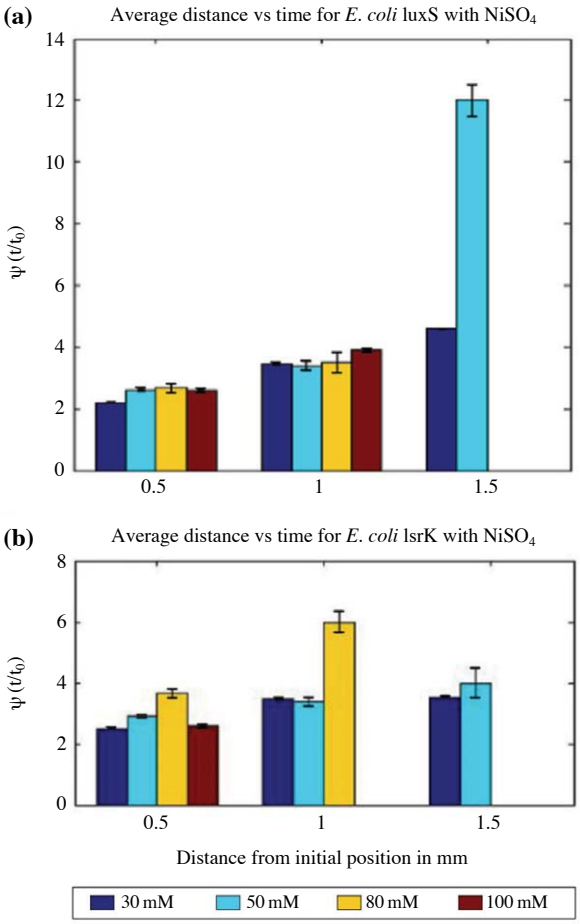

Figure 7. (a) *E. coli* luxS mut response to $NiSO_4$ and (b) *E. coli* lsrK mut response to $NiSO_4$.

(b). As $NiSO_4$ tends to repel *E. coli* cells, it was found that the amount of time required to navigate a channel was significantly higher ($\psi \gg 1$) than the normal migration time. However, we observed that the chemotactic response of *luxS* mutant to concentrations higher than 50 mM was almost non-existent. Similarly, the motility of the *lsrK* mutant ceased completely 1 mm away from the initial position in a 100 mM $NiSO_4$ gradient. These results, while seemingly counterintuitive, are not unexpected as there have been a number of studies that have reported drops in cellular movement when $NiSO_4$ concentrations were above 10 mM[15,35,36]. The Ni^{2+} ion of dissolved Nickel Sulfate has been attributed several factors such as cellular toxicity and bacterial bio-sensing, and its adsorption onto bacterial chemoreceptors is the driving force behind negative chemotaxis. Furthermore, it has been shown that as Ni^{2+} concentration increases the tumbling frequency of bacteria rises, increasing their average angular velocity but decreasing their translational motion[37]. While the

complete underling mechanism has not been fully established, it is hypothesized that the nonmotility of cells is due to disruption of metallo-regulatory proteins, such as the methyl-accepting protein Tar, at high nickel ion concentrations, which in turn inhibits motility[36,38].

Conclusions

We have demonstrated that diffusion based chemotactic behavior can be investigated in a relatively simple microfluidic devise using pneumatic micro-valve manipulation. Specifically, it was shown that the chemotactic behavior of individual bacterial species, in a chemoeffector gradient field, can be quantitatively analyzed using image processing. In separate experiments we observed the predicted the behavior of two strains of *E. coli* in the presence of increasing concentrations of known chemoeffectors. While one of the microchannels was not necessary in the experiments we conducted, as two of the channels had the same concentration chemoeffector, the three channel design allows for future more advance experiments. For example, using two inlets to introduce bacterial cells, one can evaluate the response of two groups of cells simultaneously. Devices built on this concept could utilize microchannels of shorter length to more accurately quantify the behavior of bacteria in various microenvironments, as longer microchannels would require longer times for diffusion, which would also lead to saturation of chemoreceptors. Using valves and a simple setup enables for experimental verification of positive and negative chemotaxis at a faster rate without having to deal with excessive technical difficulties. The simple triangular setup minimizes errors due to biased movement on one side, as the net movement is averaged out in left and right direction of cellular movement. Hence, this device holds wider possibility of applications in various experiments such as toxicity detection and quorum sensing research.

Materials and Methods

Bacterial strains and reagents

E. coli K-12 and its isogenic quorum sensing mutant strains (*ΔluxS* and *ΔlsrK*) were transformed with a plasmid encoding GFP (Green Fluorescent Protein). LB medium that was used to culture these strains was prepared by mixing 10 g of Tryptone, 5 g of yeast extract, 10 g of NaCl in distilled pure water, followed by autoclaving. SU-8 photoresist (PR) was purchased from MicroChem (USA). Silicon wafers (3 inches) was purchased from Wafer World (West Palm Beach, FL). The Sylgard 184 polydimethylsiloxane (PDMS) prepolymer and curing agent were purchased from Dow Corning (Newton, MA). The antibiotic ampicillin was purchased from Sigma Aldrich (St Louis, MO). The chemoattractant L-aspartate and chemorepellent nickel sulfate were also purchased from Sigma Aldrich.

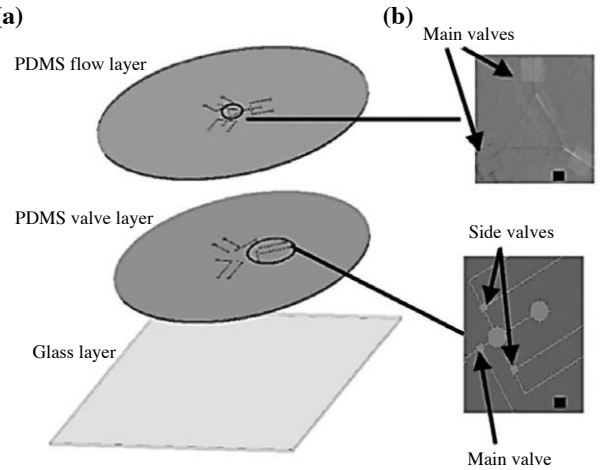

Figure 8. (a) The device has three layers: top flow layer, middle valve layer, and bottom glass substrate. Device was fabricated by using bilayer fabrication of channel and flow layer for push-up valve configuration followed by plasma treatment for attachment with glass slide. (b) Top figure shows the main experimental channel with three main valve that regulates the flow from the chambers. Scale bar 200 μm. Bottom figure shows the two side valves for inlet and outlet of each chamber. Scale bar is 400 μm.

Cultivation of *E. coli* and separation of motile cells

Each strain was incubated for approximately 10 hours at 30-32°C. Ampicillin (100 μg/mL) was added for GFP plasmid selection and retention. The cultures were aerated by gently shaking the tube at about approximately 180 rpm. Bacterial cells were removed from the incubator during the exponential phase of their growth for the experiments. Chemoeffectors were added at mid-point concentration after 5-6 hours of incubation. *E. coli* cells were then separated from the nutrient broth by centrifugation at 400 g for 10 min at room temperature, and then re-suspended in 15 mL of chemotaxis buffer (1 × PBS, 0.1 mM EDTA, 0.01 mM L-methionine, 10 mM lactic acid) with gentle shaking. This process was repeated for 4-5 times. The bacterial cells were then diluted with motility buffer (0.01 M Potassium Phosphate buffer, 0.067 M Sodium Chloride, 10^{-4} M EDTA, pH 7.5) to a concentration of ~1.5×10^8 cells /mL (determined by optical density measurements at 600 nm [OD_{600}]). Before the start of the experiment

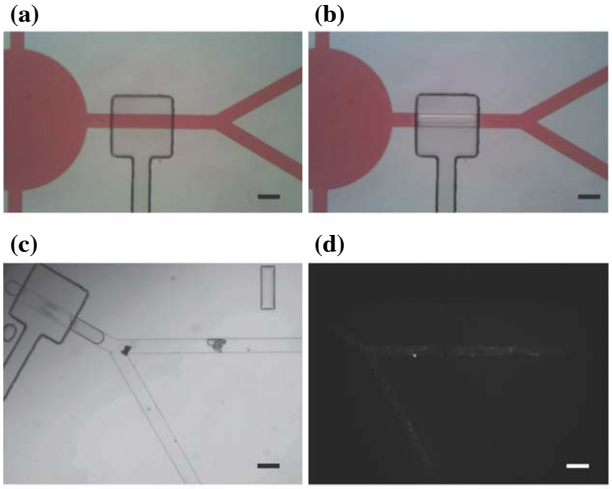

Figure 9. Valve testing using red dye (a) before and (b) after. (c) Valve in operation. At this instant the valve has just been opened and the pressure induced flow is filling the microchannels. (d) Laser induced gfp expression of *E. coli* inside the channels. Scale bar are 100 microns.

the motility was experimentally verified by pipetting a drop of bacterial cells in a cover slide and observing the motility under microscope.

Device fabrication and testing

The microfluidic device was fabricated by using multilayer soft lithography[39] as shown Figure 8. Briefly, the negative tone photoresist SU-8 was coated on the 3-inch silicon wafer followed by UV treatment (400 nm) and etching, to obtain the mold of height of ~20-30 μm. The resulting rectangular channels were used for fabricating control channels with valves by using PDMS (polydimethylsiloxane) (Dow-Corning, Cortland, NY, USA). The PDMS was mixed with curing agent in ratio (1 : 30) and spincoated onto the fabricated mold at 500 rpm for 10 sec and 3000 rpm for 30 sec. The flow layer mold was fabricated from AZ 9260 followed by UV treatment (365 nm) to obtain mold height of 25-35 μm, with valve area of 300 μm × 300 μm. The diameter of the chambers is 1 mm, and the connecting channels between the chambers are 100 μm wide. The main valves (three main valves in total) were controlled by individual channels whereas every two side-valve combination (six side valves in total) was controlled by a single microchannel. Half curing process was employed in which the two layers were semi-cured for ~1 hour at 60°C, and were aligned and thermally bonded for another 3-4 hours. It was following by treating the bonded PDMS device in plasma for 30 sec, and attaching the glass slide to it. Holes were punched using a blunt needle to insert the tubing. Pneumatic valves were then connected through Tygon tubing (Fisher Scientific International Inc., Hampton, NH, USA) to the nitrogen gas tank via valve controller. A tailored LabVIEW program was written to control the valve controller using NI DAQ board, which was connected to Nitrogen tank. The inlets and outlets were connected to the syringe pump containing their respective chemicals. The outlets were connected to the waste chamber. It is important that the tubes are submerged and as static as possible to prevent any miniscule pressure fluctuations. This was achieved by using double sided tape to attach the tubes to the substrate.

Once the device was fabricated dyes were used to test the valves as shown in Figure 9(a) and (b). By using the LabVIEW controlled custom program, the valves were able to be turned on and off instantaneously. A simple experiment was conducted to see the performance of device in which the channels was filled with GFP-labelled *E. coli* cells, and they were allowed to diffuse. The argon ion laser was used to excite the GFP protein. Using high resolution camera, the images were captured as shown in Figure 9(d).

Acknowledgements We acknowledge the invaluable contributions of A. Agung Julius and Cynthia Collins for access to their expertise, advice, and experience in understanding bacteria. This work was funded by Army Research Office (W911NF-11-1-0490) award to M.J. Kim and by NRF (National Research Foundation) Public Welfare & Safety Research Program award in Korea (2012-00065 22) to S. Park.

References

1. Whitesides, G.M. The origins and the future of microfluidics. *Nature* **442**, 368-373 (2006).
2. Kim, M.J. & Breuer, K.S. A Selective Mixing in Microfluidic Systems Using Bacterial Chemotaxis. in *ASME* 277-282 (2005).
3. Kim, S., Kim, H.J. & Jeon, N.L. Biological applications of microfluidic gradient devices. *Integr. Biol.* **2**, 584-603 (2010).
4. Weibel, D.B. & Whitesides, G.M. Applications of microfluidics in chemical biology. *Curr. Opin. Chem. Biol.* **10**, 584-591 (2006).
5. Sia, S.K. & Whitesides, G.M. Microfluidic devices fabricated in poly (dimethylsiloxane) for biological studies. *Electrophoresis* **24**, 3563-3576 (2003).
6. Weibel, D.B., DiLuzio, W.R. & Whitesides, G.M. Microfabrication meets microbiology. *Nat. Rev. Microbiol.* **5**, 209-218 (2007).
7. Zare, R.N. & Kim, S. Microfluidic platforms for single-cell analysis. *Annu. Rev. Biomed. Eng.* **12**, 187-201 (2010).
8. Li, J. & Lin, F. Microfluidic devices for studying che-

motaxis and electrotaxis. *Trends Cell Biol*. **21**, 489-497 (2011).
9. Meyvantsson, I. & Beebe, D.J. Cell culture models in microfluidic systems. *Annu. Rev. Anal. Chem*. **1**, 423-449 (2008).
10. Ahmed, T., Shimizu, T.S. & Stocker, R. Bacterial chemotaxis in linear and nonlinear steady microfluidic gradients. *Nano Lett*. **10**, 3379-3385 (2010).
11. Keenan, T.M. & Folch, A. Biomolecular gradients in cell culture systems. *Lab Chip* **8**, 34-57 (2007).
12. Diao, J. *et al*. A three-channel microfluidic device for generating static linear gradients and its application to the quantitative analysis of bacterial chemotaxis. *Lab Chip* **6**, 381-388 (2006).
13. Wadhams, G.H. & Armitage, J.P. Making sense of it all: bacterial chemotaxis. *Nat. Rev. Mol. Cell Biol*. **5**, 1024-1037 (2004).
14. Eisenbach, M. Bacterial Chemotaxis. in *eLS* (John Wiley & Sons, Ltd, 2001).
15. Kim, M.J. & Breuer, K.S. Controlled mixing in microfluidic systems using bacterial chemotaxis. *Anal. Chem*. **79**, 955-959 (2007).
16. Phuyal, K. & Kim, M.J. Mechanics of swimming of multi-body bacterial swarmers using non-labeled cell tracking algorithm. *Phys. Fluids B* **25**, 011901 (2013).
17. Berg, H.C. Motile behavior of bacteria. *Phys. Today* **53**, 24-30 (2000).
18. Darnton, N.C., Turner, L., Rojevsky, S. & Berg, H.C. Dynamics of bacterial swarming. *Biophys. J*. **98**, 2082-2090 (2010).
19. Ford, R.M. & Harvey, R.W. Role of chemotaxis in the transport of bacteria through saturated porous media. *Adv. Water Resour*. **30**, 1608-1617 (2007).
20. Paguirigan, A.L. & Beebe, D.J. Microfluidics meet cell biology: bridging the gap by validation and application of microscale techniques for cell biological assays. *BioEssays* **30**, 811-821 (2008).
21. Jeon, N.L. *et al*. Neutrophil chemotaxis in linear and complex gradients of interleukin-8 formed in a microfabricated device. *Nat. Biotechnol*. **20**, 826-830 (2002).
22. Chung, B.G. *et al*. A gradient-generating microfluidic device for cell biology. *J. Vis. Exp*. **7** (2007).
23. Jeon, N.L. *et al*. Generation of solution and surface gradients using microfluidic systems. *Langmuir* **16**, 8311-8316 (2000).
24. Cheng, S.-Y. *et al*. A hydrogel-based microfluidic device for the studies of directed cell migration. *Lab Chip* **7**, 763-769 (2007).
25. Haessler, U., Kalinin, Y., Swartz, M.A. & Wu, M. An agarose-based microfluidic platform with a gradient buffer for 3D chemotaxis studies. *Biomed. Microdevices* **11**, 827-835 (2009).
26. Atencia, J. & Beebe, D.J. Controlled microfluidic interfaces. *Nature* **437**, 648-655 (2005).
27. Beebe, D.J., Mensing, G.A. & Walker, G.M. Physics and applications of microfluidics in biology *Annu. Rev. Biomed. Eng*. **4**, 261-286 (2002).
28. Mengeaud, V., Josserand, J. & Girault, H.H. Mixing processes in a zigzag microchannel: finite element simulations and optical study. *Anal. Chem*. **74**, 4279-4286 (2002).
29. Studer, V. *et al*. Scaling properties of a low-actuation pressure microfluidic valve. *J. Appl. Phys*. **95**, 393-398 (2003).
30. Kamholz, A.E., Weigl, B.H., Finlayson, B.A. & Yager, P. Quantitative analysis of molecular interaction in a microfluidic channel: the T-sensor. *Anal. Chem*. **71**, 5340-5347 (1999).
31. Erickson, D. Towards numerical prototyping of labs-on-chip: modeling for integrated microfluidic devices. *Microfluid. Nanofluid*. **1**, 301-318 (2005).
32. Berg, H.C. *E. coli in Motion*, (Springer, 2004).
33. Alon, U., Surette, M.G., Barkai, N. & Leibler, S. Robustness in bacterial chemotaxis. *Nature* **397**, 168-171 (1999).
34. Adler, J. A method for measuring chemotaxis and use of the method to determine optimum conditions for chemotaxis by Escherichia coli. *J. Gen. Microbiol*. **74**, 77-91 (1973).
35. Mao, H., Cremer, P.S. & Manson, M.D. A sensitive, versatile microfluidic assay for bacterial chemotaxis. *PNAS* **100**, 5449-5454 (2003).
36. De Pina, K., Desjardin, V., Mandrand-Berthelot, M. -A., Giordano, G. & Wu, L.-F. Isolation and Characterization of thenikR Gene Encoding a Nickel-Responsive Regulator in Escherichia coli. *J. Bacteriol*. **181**, 670-674 (1999).
37. Borrok, D., Borrok, M.J., Fein, J.B. & Kiessling, L.L. Link between chemotactic response to Ni^{2+} and its adsorption onto the Escherichia coli cell surface. *Environ. Sci. Technol*. **39**, 5227-5233 (2005).
38. Macomber, L. & Hausinger, R.P. Mechanisms of nickel toxicity in microorganisms. *Metallomics* **3**, 1153-1162 (2011).
39. Unger, M.A., Chou, H.-P., Thorsen, T., Scherer, A. & Quake, S.R. Monolithic microfabricated valves and pumps by multilayer soft lithography. *Science* **288**, 113-116 (2000).